MODELLING HEAT AND MASS TRANSFER IN GAS-SOLID FLUIDIZED BEDS USING THE TWO-FLUID GRANULAR TEMPERATURE APPROACH

by

Jefferson Luís Melo de Almeida Gomes

(B.Sc. M.Sc.)

A thesis submitted in fulfillment of the requirement for the degree of Doctor of Philosophy of the University of London and the Diploma of the Imperial College London

Imperial College London

University of London

January 28, 2004

To my parents,

José and Janete,

and my brother and sister,

Alexandre and Daniela.

Love and Thanks.

To my lovely wife
Liliam
and to the greatest
football team in the world
Botafogo Futebol e Regatas.

You look up when you desire to be exalted.
And I look down, because I am exalted.
Who among you can at the same time laugh and be exalted?
He who climbs upon the highest mountains laughs at all tragedies, real or imaginary.
Friedrich Nietzsche

Nil sapienticie odiosius acumine nimio

Sêneca

A thing is not proved just because
no one has ever questioned it.
What has never been gone into impartially
has never been properly gone into.
Hence scepticism is the first step toward truth.
It must be applied generally,
because it is the touchstone.

Denis Diderot

Aknowledgements

I would like to thank my supervisor, Dr. Christopher C. Pain, for his help, enthusiasm and guidance during this work. Also thanks my co-supervisors, Dr. Cassiano R. E. de Oliveira, for the strong support during all these years, and Professor Anthony J. H. Goddard, for his wise guidance.

Thanks to my groupmates: Lal Akash Lal, who gave me strong support in my first hard and cold days in the UK; Gerard Gorman, who worked very hard to solve many of the computational problems I had and became a good friend; Geeta Chari, who spent several hours helping me to understand the physics associated with multiphase flow and reviewing this work; Matthew Eaton, who has been giving me strong support since I arrived; Sabu Shahdatullah, Manuela Duglio and Angelo Maggiore, who with their great sense of humor were essential to my sanity; Dr. Elsa Aristodemou, who helped me to review this work. I also want to thank Mr Adrian P. Umpleby and Dr. Kemal Ziver, who helped with several parts of this work.

A special thanks to my wife, Liliam S. Costa, who has supported me in all the moments.

This work has been funded in part by CAPES/Brazil and by PROCASE-UERJ/Brazil.

Abstract

In this work, gas-solid fluidization is numerically investigated using the Two-Fluid Model (TFM), in which both gas and solid phases are modelled as fully inter-penetrating continua. In the TFM framework, each phase is described by a set of conservative equations with interaction terms representing the coupling between the phases. The set of conservative equations, i.e. continuity, momentum, fluctuation and thermal energies are solved by the computational fluid dynamics code, *FLUIDITY*. Particle phase thermal diffusivity is modelled using kinetic theory for dry granular flows. The resulting heat transfer model has the advantage of maintaining consistency with the overall model which is based on the granular temperature approach.

The modelled heat transfer coefficients are compared with both experimental results available in the literature and with analytical solutions. The overall model is used here to investigate a number of complex particle fluidization problems such as: a novel fluidized bed nuclear reactor, particle fluidization by rapidly vaporizing water, and particle cluster formation in risers and bubbling fluidized beds. Since the dynamics of these systems are often chaotic, the simulations are compared in a statistical sense to available experiments as part of the model validation exercise.

Contents

List of Tables

List of Figures

Notation

v	velocity	m.s^{-1}
t	time	s
x	spatial coordinate	m
p	pressure	Pa
g	gravitational force	m.s^{-2}
T	thermodynamic temperature	K
C	heat capacity	J.(kg.K)$^{-1}$
q	flux of fluctuation energy	kg.s^{-3}
$\overline{MW}$	molecular weight	kg.kgmol^{-1}
C_D	drag coefficient	
h	fluid-particle heat transfer coefficient	$W.m^{-2}.K^{-1}$
V	volume	m^3
$\overline{V}$	molar volume	m^3.gmol^{-1}
$\overline{A}$	area	m^2
e	restitution coefficient	
H	heat transfer coefficient	$W.m^{-2}.K^{-1}$
r	radius	m
n	normal	m
d	diameter	m

Greek letters

ε	volume fraction

ρ	density	kg.m^{-3}
β	interphase momentum transfer coefficient	kg.m^{-3}.s^{-1}
τ	viscous stress tensor	N.m^{-2}
Γ	frictional force exerted on the wall by the phase	N.s.m^{-4}
κ	thermal conductivity	W.(m.K)$^{-1}$
α	volumetric interphase heat transfer coefficient	W.m^{-3}.K^{-1}
Ω	volumetric wall-phase heat transfer coefficient	W.m^{-3}.K^{-1}
Θ	granular temperature	m^{2}.s^{-2}
γ	collisional energy dissipation	kg.m^{-1}.s-3
μ	viscosity	kg.m^{-1}.s^{-1}
ν	radial distribution function	
Υ	thermal energy source	J.s^{-1}
$\overline{\mu}$	friction coefficient	

Superscripts

mp	maximum packing condition
o	initial conditions
inl	inlet conditions
gas	pure gas
sol	pure solid

Subscripts

mf	minimum fluidization conditions
mb	bubbling conditions
f	fluid phase
s	solid phase
w	wall
i , j	coordinates index
p	particle

gas	pure gas
sol	pure solid
T	total
$susp$	suspension
cyl	cylinder
$emul$	emulsion

Constants

R	universal gas constant	8.31451 J.(gmol.K)$^{-1}$

Dimensionless Numbers

Particle Reynolds	$Re_p = \frac{\varepsilon_s \rho_f \left\|v_f - v_s\right\| d_s}{\mu_f}$
Prandtl	$Pr = \frac{C_f}{\mu_f}\kappa_f$
Nusselt	$Nu = \frac{h_{fs} d_s}{\kappa_f}$
Biot	$Bi = \frac{h_{fs} d_s}{\kappa_s}$

Part I

Fundamentals

Chapter 1

Introduction

1.1 Fluidization and Fluidized Beds

Fluidization can be defined as the process by which solid particles or liquids (either homogeneous or heterogeneous) are transformed into a fluid-like state via suspension in a fluid (gas or liquid) [4]. This work focuses on gas-solid fluidization in which the gas phase is assumed to behave as an ideal gas in thermodynamic equilibrium.

If the gas is pumped upwards through a granular bed at a low flow rate, the fluid percolates through the pores with no perturbation of the bed height, and it is called a fixed bed process. However, if the flow rate is high enough to expand the bed by establishing a mean-free distance between the particles (Figure 1.1), and these particles are supported by drag forces due to the fluid phase, then the bed is considered to be at minimum fluidization. This fluid flow velocity is known as minimum fluidization velocity (u_{mf}), and can be estimated by several empirical correlations, such as the Ergun [5] and the Thonglimp [6] equations.

Bubbles and channels start to appear in the porous medium as the fluid flow rate rises beyond incipient fluidization conditions. At this stage (bubbling regime), the resultant bed height is slightly higher than at minimum fluidization. The bubbles generated during fluidization rise through the bed, increasing the mixing. However, as they move upwards, the bubbles become larger. The flow is slugging if either the fluid flow rate is increased or the bed diameter is decreased (Figure 1.1(C)), i.e., particles rise in the wake of large (and

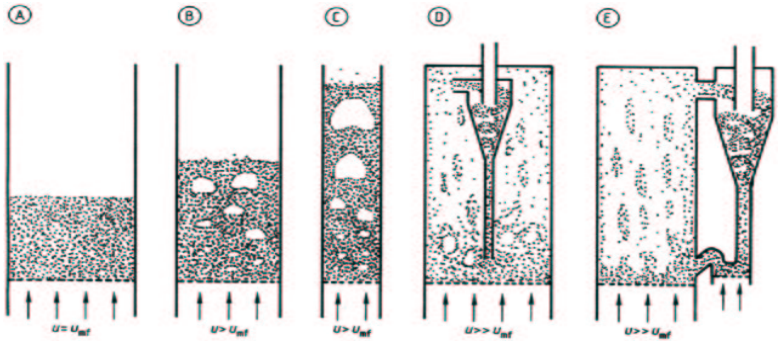

Figure 1.1: Fluidization: initially (A) the gas phase rises through the porous media with no perturbation on the time-averaged bed height, however as the superficial gas velocity rises beyond the minimum fluidization velocity (B-C), bubbles start to be formed and move upwards. (D-E) show turbulent flows that occur with large superficial gas velocity.

coalesced) bubbles and fall smoothly along the wall.

Fluid-particle flows can also be classified as either dilute or dense [7], although it is not possible to establish a sharp distinction between them. A flow is said to be dilute when the particle motion is controlled by surface and body forces on the particles. However, the particle motion in dense flows is mainly controlled by particle-particle collisions and interactions. In this sense, dilute flows can be observed in risers, in which, after the initial loading, and as the stream becomes increasingly dense, the flow reaches a quasi-steady state regime and is mainly controlled by particle-walls collisions and gravitational forces. However, particle-particle interactions, parameterized by collisional friction and particle-particle restitution coefficients, also play an important role in the fluidization regime [8, 9, 10].

Fluidized beds can be defined as vessels containing either granular particles or liquids, which are fluidized by an upward gas-flow. When the inlet gas velocity reaches the so-called bubbling velocity (u_{mb}), bubbles start to rise through the bed, enhancing mass and heat transfer rates due to the intense mixing. In addition, for gas-solid fluidization, granular particles move downward in the wall regions and improve the gas-particle mixing by the formation of vortices in the lower region of the bed [11, 12].

1.2 Industrial Applications

Fluidization processes are widely used by a great assortment of industries worldwide and represent a trillion dollar industry [13, 4]. They are currently used in separation, classification, drying and mixing of particles, chemical reactions and regeneration processes. Fluidized beds play an important role in the chemical and petrochemical industries, especially in the production of chemicals such as ethylene, propylene, HDPE, LDPE, LLDPE and benzene. They are also used in power generation from the combustion of coal [14, 15] or biomass gasification [16, 17].

Fluidized beds are perhaps best known for their use in fluid catalytic cracking (FCC) processes, where 'heavy fractions' of oil (i.e. hydrocarbons of high molecular weight) are broken up into fractions of lower molecular weight by the action of a catalyst [18]. The heavy fractions, fed from the bottom boundary of riser crackers, Figure 1.2, is vaporized when in contact with hot high-activity zeolite catalysts. The mixture of oil vapors and cracking gas transports the catalyst up through the riser. From there, the solid catalysts are recovered (through a set of strippers and regenerators) and fed back into the riser. Due to the short contact time (on the order of a few seconds) and the narrow gas residence-time, the high activity of the zeolite catalyst is optimally utilized and a higher gasoline yield is achieved [19].

Gas phase technologies, rather than conventional liquid slurry processes, have been used to produce polyolefins (PO), a second generation set of petrochemicals used in industrial processes. These technologies involve the use of Ziegler-Natta catalysts of high activity and selectivity in either fluidized bed reactors, or in vertical or horizontal agitated vessels [20]. For example, in the gas-phase polymerization of ethylene in fluidized beds using the Unipol process (Figure 1.3), ethylene, butene and hexene fluidize fine grade of catalysts. The exothermic reaction occurs on the catalyst surface and yields a granular product with diameter ranging from 250 to 1000 μm. Such technologies, developed in the early 1980's, helped to boost research in many other fluidization processes, such as the production of chlorine [21].

Due to their excellent mixing and heat transfer capabilities, fluidized bed furnaces

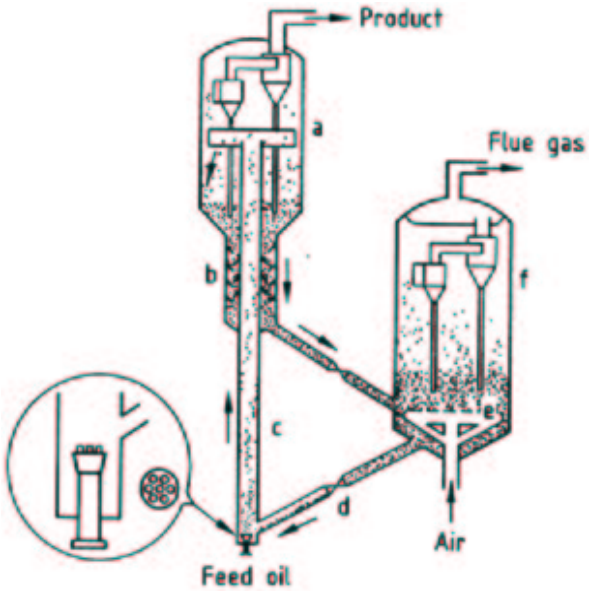

Figure 1.2: Riser cracking process (UOP system [1]): (a) reactor, (b) stripper, (c) riser, (d) slide valve, (e) air grid and (f) regenerator.

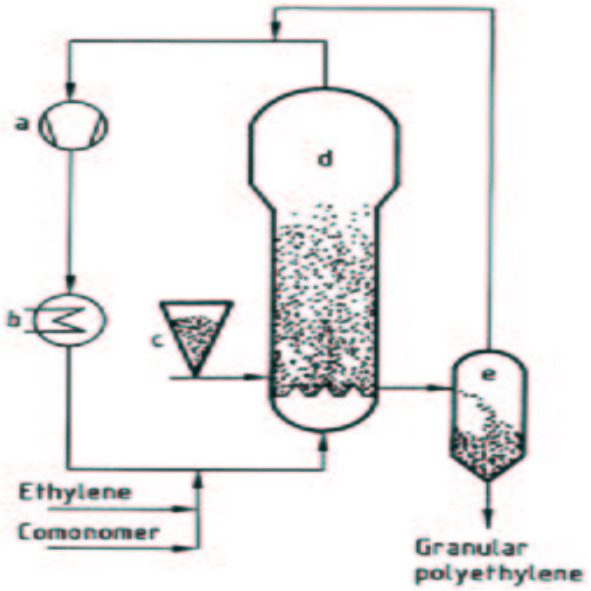

Figure 1.3: Gas-phase polymerization of ethylene (Unipol process [1]): (a) compressor, (b) cooler, (c) catalyst feed hopper, (d) reactor and (e) separator.

have also been used in coal combustion at low temperature ($\approx$ 850 ^{o}C). This allows a high efficiency in the power plants [1] due to the optimal use of coal with low production/emission of nitrogen oxides. Other important industrial products obtained in fluidization processes are phthalic anhydride [22], phthalonitrile, maleic anhydride, and melamine [1] (see also [19, 4, 23]).

Fluidized beds have also been used in biotechnological processes (liquid-solid-gas systems) since the early 80's. Due to their intense mixing and larger capacity per unit volume than fixed beds, aerobic and anaerobic wastewater treatments have taken place in fluidized beds [1, 22]. They have also been used as fermenters and in the biogas production [24, 25].

The intensive use of fluidized bed reactors in industrial processes is due to their particular properties:

(i) uniform temperature distribution due to intense solid-fluid mixing

(ii) high heat transfer coefficient between the bed and energy source

(iii) large solid-fluid area due to the small size of the particles

(iv) smooth transport of solids due to liquid-like behavior of the fluidized bed

(v) uniform solid product in batch processes due to the intense mixing

However, although these advantages seem very encouraging, the drawbacks that provide a strong motivation for further development of new techniques are:

(i) difficulty in scaling-up of fluidized bed reactors

(ii) erosion of internals that work as heat exchangers

(iii) eventual formation of agglomerates which may decrease efficiency

(iv) lower chemical conversion due to nonuniform solids residence time

(v) expansive solids separation due to solids entrainment by fluidizing gas

Although these disadvantages may impose serious restrictions to the use of fluidized beds as reactors due to eventual low process efficiency, research works focused on new materials and fluid dynamics may overwhelm such disadvantages. For example, research in fluidized bed combustors operating at pressures of up to 1.5 MPa indicates that the efficiency may rise to up to 45 $\%$ [1]. The IEA's pressurized fluidized bed boiler (PFBC) demonstration unit [26] will be capable to produce approximately 80 MWe, while larger units in operation in Japan reached 360 MWe. Although in this process, the emission of N_2O is increased and thus new chemical filters are necessary, SO_2 and NO_x emissions were reduced.

A wide range of wastes, such as municipal solid wastes, sewage sludge, petroleum wastes and others, have been incinerated in fluidized beds [27]. Research works in this area have led to models in which heavy metals in the ashes of the resulting waste incinerations need to be dealt with. Zhou *et al.* [28] investigated the dynamics associated with the vaporization of $CdCl_2$-alumina in a lab-scale gas-solid fluidized bed operating at 850^oC. In this work, they studied the mass transfer due to the vaporization of cadmium salt chemically linked to alumina, and the elimination of this heavy metal from the ashes. However, further chemical reactions between the alumina surface inhibited the full $CdCl_2$ vaporization.

Therefore, the optimization of the parameters used in these processes has received a great deal of attention from the scientific community [29, 8]. Moreover, knowledge of fluidization hydrodynamics is crucial for the development of new technologies. This has provided the motivation for the development of several commercial and academic computational fluid dynamics (CFD) codes.

Thus, although fluidized beds have been receiving a great deal of attention from the scientific community due to their impressive capabilities as reactors and mixers, many questions relating to the dynamics, heat and mass transfers are still to be answered. One of the aims of this research work is to address issues regarding heat transfer, phase exchange and flow regime characterization.

1.3 Multiphase Flow Models

Although the use of fluidized beds in industrial applications dates from the early 1920's, the development of zeolites as a more active and selective catalyst in the 1960's, boosted the use of bubbling and circulated fluidized beds in order to improve the performance of FCC processes. Although the hydrodynamics of gas-solid fluidized beds had been exhaustively studied by many researchers, only in the last 10 years could computational resources be fully applied to the development of numerical techniques that would allow the modelling of such complex systems.

Two types of numerical models were developed to model complex multiphase flows: the discrete element method (DEM) and the continuous method. In the first, originally developed by Cundal [30, 31] to study rock mechanics, particles are individually tracked through the domain and all interparticle forces due to collisions or stress are modelled. Thus each particle is modelled in interaction with the surroundings by the Newtonian law of motion.

This model was modified by Tsuiji *et al.* [32] for granular flows. The contact forces between the particles, expressed as spring, dash-pot and friction slider forces, are modelled. Particle attraction is also a function of the plasticity of the contact and the Young's modulus of the particles, giving rise to the concept of soft and hard granules. Furthermore, the rotation associated with the particles during their motion and collisions is also considered for the soft granules.

By contrast, the two-fluid model (TFM), as a continuous method, treats both phases as an interpenetrating continuum. Having been used in this work, it is described in Chapter 2. The TFM model is generally less computationally demanding than the DEM and has thus been extensively used by the CFD community (MFIX, CFX, FLUENT, and others [33, 34, 35, 18]), although DEM models have been attracting attention [20, 32, 36] due to the continued increase in computational power enabling the fluidization of large number of particles to be modelled.

In the two-fluid model, both phases are represented by transport equations for the conservation of mass, momentum, and energy in order to calculate the respective volume

fractions, velocities, pressure and temperatures. The TFM requires additional closure laws to describe the rheology of the particulate phase. These closure laws are based on the assumptions of kinetic theory for dry granular flows. Comprehensive reviews of kinetic theory of granular flows can be found in Drew and Passman [37], Gidaspow [38], Soo [39] and Kuipers *et al.* [40].

The particle-particle collisions and particle-wall interactions can be modelled through the solid stress. In this case, the solid stress is described as a function of the solid velocities, the particle binary collisions and the solids pressure. However, the turbulence requires separate treatment, for example by the $k - \varepsilon$-model [38]. Ding and Gidaspow [41] developed a model to predict the granular viscosity and stress for dry flows and introduced the concept of granular temperature as a measure of the agitation of particles. Granular temperature provides a link between kinetic theory and traditional fluid mechanics.

1.4 Chaos Theory

Despite the extensive efforts to improve the results obtained from numerical simulations by the development of new numerical techniques, comparisons of such results and those obtained from experiments are still an issue, since only statistical quantities can be properly compared [42, 43, 44, 45]. As the granular flow in fluidized beds is chaotic, dynamic analysis has been applied to either voidage or pressure fluctuations to identify the flow regime.

A characteristic chaotic feature is the extreme sensitivity to changes in the initial conditions, while the dynamics is constrained to a finite region of the space state called a strange attractor[1]. Chaos has been identified in several systems such as simple electric circuits [48], macroeconomics [46], turbulent flows [49] and biological systems [50]. In

[1]The basic idea behind an attractor is that a dynamic system will tend toward certain states as evolving in time. This concept is very useful when one applies it to a set of differential equations whose solutions seem to approach the same set in phase space, i.e., the attractor. The solutions will never, indeed, approach the same point. Even if their initial conditions are very close to one another, they will typically separate rapidly in time. This is known as the *chaotic* behavior of differential equations with a sensitive dependence

the last, Small *et al.* [50] used surrogate data and correlation dimension techniques to show that the dynamics observed in simulated ventricular fibrillation signals is similar to that observed in patients suffering ventricular fibrillation.

The study of chaotic systems may be divided into three areas: identification of chaotic behavior, modelling and prediction, and control. The identification of chaotic behavior is important to distinguish it from stochastic processes. In addition, it may help to estimate the degree of freedom of a system. The investigation of the complexity of underlying chaotic systems and the identification of the strange attractors, i.e., state space representations, associated with the chaotic behavior may lead to predictions of both the behavior of the system and the dynamics associated with this attractor in a short-term sense. In this sense, neural networks and Kriging techniques have been extensively used by a number of researchers [51, 52].

In systems that present chaotic behavior, a small perturbation in the input signal may lead to large effects in the output signal. Therefore, in order to control chaotic systems, it is necessary to predict how systems will react to perturbations. In Chapter 5, the chaotic dynamics associated with a conceptual nuclear fluidized bed is investigated. The embedded dimension of the strange attractor associated with the fission rate is used to predict the fission rate and temperature fluctuations in a short-term sense. Further developments of this work may include reliable feedback controlling techniques. In addition, flow regime and macrostructures of the fluid flow are investigated through deterministic chaos theory in Chapters 5, 8 and 9.

1.5 Heat and Mass Transfer in Fluidized Beds

Fluidized beds exhibit a uniform temperature distribution due to the vigorous mixing provided by the random motion of the bubbles [22, 53]. Since the particle surface area is very large, fluid-to-particle heat and mass transfer is rarely a limiting factor in the design and control of fluidized bed reactors as the heat transfer between surfaces (working as thermal source or sink) and the fluid-solids is. Therefore, the knowledge of these heat

on initial conditions [46, 47].

transfer rates is of fundamental importance in the design and control of fluidized-bed reactors, if the aim is to optimize the performance of the internals used for cooling and heating of the fluid-particle system.

However, so far there is no complete general theory on the heat and mass transfer of fluidized beds. Khan & Elkamel [54] summarized several of the main fluid-particle models available in the literature. Most of these models are based on the assumption of a thermal boundary layer along the thermally active surface, which is continuously perturbed by the motion of the gas-particle emulsion. The interaction between this emulsion and the boundary layer is the mainly responsible for the thermal diffusion throughout the domain. Kunii & Levenspiel [4] extended this model to gas-solid fluidized beds operating under bubbling conditions in which bubbles by themselves make a neglible contribution to the heat transfer from internals as the particle concentration is very small. The main contribution is due to the mixing that they promote of the emulsion phase in their wake. Chapter 4, the influence of the bubbles' wake on the emulsion-surface heat transfer in gas-solid fluidized beds is investigated.

Several correlations for the calculation of the Nusselt and Sherwood dimensionless numbers are reported in the literature. Since these correlations are mainly based on experimental investigations performed under laboratory conditions, they may be different to the situation in large-scale reactors. Haid *et al.* [55] reviewed most of the correlations used for liquid-solid fluidized beds. They also investigated the influence of scaling parameters, such as bed geometry, flow velocities, and fluid and solid thermo-physical properties, on some of these empirical correlations and compared the predictions obtained with experimental data. Gunn [56] studied the heat and mass transfer in gas-solid fixed and fluidized beds operating in a wide range of fluid velocities and porosities. He developed a theoretical correlation that expresses the heat exchanged between particles and fluids and its interaction with conduction and convection processes. This expression satisfies the asymptotic condition that the Nusselt number vanishes as the porosity tends to unity, which is a natural condition for particle systems.

Molerus *et al.* [57, 58] investigated the heat exchanges between immersed surfaces and fine particles in the bubbling regime. They concluded that the particle motion in

fluidized beds enhances the heat transfer by constantly renewing particles in the thin thermal boundary layer, as previously reported by Wasmund & Smith [59] and Mickley & Fairbanks [60]. They also proposed an expression for predicting the global heat transfer coefficient as a function of the Archimedes dimensionless number. This expression mirrors the dependence of the heat transfer coefficient on the superficial gas velocity. They observed that for flows operating with fine particles, the solid phase is mainly responsible for transporting heat between walls and bed, whereas gas convective transport is the main mechanism dominating the heat transfer of coarse particles. For intermediate particle sizes, the total heat transfer attains a maximum due to the superposition of both transport mechanisms (see also [61]).

Sunderesan & Clark [62] measured the time-varying surface temperature of tubes immersed in a bubbling fluid-particle solution. They used particles of several dimensions and materials, and observed a strong correlation between the bubbles frequency and the heat transfer, i.e., as the number of bubbles increases, hot particles located at the cylinder surface are replaced by a fresh emulsion of particles, enhancing the heat transfer. Similar behavior occurs in the simulations described in Chapter 3.

The wall-to-bed heat transfer mechanism was numerically investigated by Kuipers *et al.* [63] in 2-D geometries. They observed that heat flux is induced by the rising of bubbles near the wall region, which provokes the displacement of hot particles by fresh particles. These 'cold' particles are mainly dragged in the bubbles' wake. A lab-scale fluidized bed with a horizontal heated cylinder was used by Schmidt & Renz [35, 34] to study the heat flux into the particle-fluid emulsion. Both the experiments and numerical simulation focused on the flow behavior around the obstacle during the rising of bubbles. They observed that the displacement of the bubbles in the vicinity of the cylinder and the subsequent formation of a dilute emulsion around it was a consequence of the rising bubbles' wake. This behavior led to an enhancement of the heat transferred to the emulsion phase, which agrees with measurements performed by Hsiau [64].

The heat flux mechanisms investigated by Kuipers *et al.* [63] and Schmidt & Renz [35, 34] are based on the so-called renewal model [54, 60, 5] which states that the heat is transferred by 'packets' of the emulsion phase which are periodically replaced from

the source/sink of energy by the action of bubbles. The bubbles would thereby act as a perturbation in the thermal boundary layer, inducing an 'unsteady' state heat transfer regime. In the calculation of the thermal diffusion in the emulsion phase, Kuipers *et al.* used an empirical expression derived by Zeher & Schlunder [65] which takes into account only the material properties of an imaginary cylinder composed of an emulsion of the particle and fluid phase. Schmidt & Renz [35, 34] extended the model used by Kuipers *et al.* to take into account, through the granular temperature, particle collisions and agitation during the flow . They compared the heat transfer and hydrodynamics results obtained from the empirical expression due to Zeher & Schlunder with the results obtained by using an expression based on the granular temperature [66]. The results were indeed, very encouraging and agreed with experiments. Hsiau [64] studied the thermal diffusion in granular flows using the analogy between inelastic particle collisions and kinetic gas theory (see also [67]). He reported that a maximum thermal diffusity is obtained at a solid volume fraction of approximately 0.25 due to the large mean free path between particles, associated with a large collisional probability function.

The model presented in Chapter 3 is based on the granular temperature as a function of agitation of the particles, indicating how strong the mixing in the bed is. The hydrodynamics and heat transfer coefficients obtained from two expressions proposed by Hunt & Natarajan [66, 68] are investigated and compared with experiments. The numerical results obtained from one of this expressions agreed with experiments available in the literature. The heat transfer model presented here is consistent with the overall model which does not rely upon empirical correlations. Numerical experiments were carried in 2-D and 3-D geometries (Chapters 3 and 4) to investigate the surface-to-bed heat transfer mechanisms.

1.6 Objectives

The main aim of this work is to investigate the heat and mass transfer in fluidized beds using the two-fluid granular temperature model. In order to achieve this aim, the set of conservative equations is solved using a high-resolution method which is globally second order accurate in space and time. The thermal diffusion is considered to be a function

of the granular temperature. This ensures the consistency of the overall model which is based on the kinetic theory for dry granular flows. The heat transfer coefficients obtained from numerical simulations are validated by comparing them with experiments available in the literature and with the analytical solution of a simplified thermal energy equation.

The hydrodynamics of dense (bubbling and slugging fluidized beds) and dilute (risers) flows are also investigated through chaos theory. The flow behavior qualitatively agrees with experiments. The confidence in the model leads to the investigation of a difficult numerical experiment, in which, the flow and fission rate behavior of a conceptual nuclear fluidized bed operating under high pressure (60 bar) is studied. A simplified kriging interpolation of the surface underlying the dynamics described by the strange attractor associated with the fission rate is proposed to predict the evolving temperature in the short-term.

In addition, a model for phase exchange in the TFM framework is proposed. In this 'false' three-phase model, pressure and temperature induce the vaporization and condensation of water-steam accordingly. This phase change is controlled by a mixed theoretical-experimental equation of state. This model may be extended to other fluids by choosing an appropriate equation of state.

1.7 Outline of the Thesis

This thesis is divided into four parts as follows. In the Fundamentals (Chapter 2), the two-fluid model used in this work to describe the fluid-particles flows in fluidized beds is summarized. In Part II, the heat and mass transfer is numerically investigated. This part is subdivided into a validation of the model presented in this work (Chapters 3, 4 and 6), investigation of heat transfer mechanisms in dense flows (Chapters 3 and 4) and applications and flow regime identification through chaos theory (Chapters 5 and 7). Investigations concerning fluid hydrodynamics, flow macrostructure, grid convergence and cluster motion are described in Part III (Chapters 8 and 9). Conclusions are drawn .

Chapter 2

The Two-Fluid Granular Temperature Model

2.1 Introduction

Two types of numerical models were developed to model complex multiphase flows: the discrete element method (DEM, based on the Eulerian-Lagragian approach) and the continuous method (based on the Eulerian-Eulerian approach). In the first, originally developed by Cundall *et al.* [30, 31] to study rock mechanics, particles are individually tracked through the domain and all interparticle forces due to collisions or stress are modelled. This model was modified by Tsuji *et al.* [32] for granular flows. The contact forces between the particles are modelled, expressed as spring, dash-pot and friction slider forces. Particle attraction is also a function of the plasticity of the contacts and the Young's modulus of the particles, producing the concept of soft and hard granules. Furthermore, the rotation associated with the particles during their motion and collisions is also considered for the soft granules.

However, the two-fluid model (TFM), as a continuous method, models both phases as an interpenetrating continuum. The TFM model is generally less computationally demanding than the DEM and has thus been extensively used by the CFD community, eg. MFIX, CFX, FLUENT, and others [10, 33, 34, 35]. DEM models have been attracting at-

tention [69, 20, 32, 36] due to the development of more powerful computational resources which enable modelling the fluidization of a large numbers of particles.

The TFM's require additional closure laws to describe the rheology of the particulate phase. These closure laws are based on the assumptions of kinetic theory for dry granular flows [37, 38, 40]. Ding & Gidaspow [41] developed a model to predict the granular viscosity and stress for dry flows, and introduced the concept of granular temperature as a measure of the agitation of particles. Granular temperature provides a link between kinetic theory and traditional fluid mechanics.

2.2 Conservative Equations

In the two-phase model, mass, momentum and thermal energy balances are described for each phase. Moreover, as the average fields of one phase are dependent on the other phase, interaction terms naturally appear in the balance equations, representing the momentum and thermal energy transferred between the phases. The full derivation of these balance equations can be found in [70, 71].

This continuum representation of the solid phase requires additional closure laws to describe the rheology of the fluidized particles. Several empirical correlations were suggested [5] to calculate the solid viscosities and the normal solid stress. However, as a more consistent way to obtain these parameters was necessary, Jenkins and Savage [72] and Ding and Gidaspow [41] derived these rheological parameters by describing the solid phase as a non-interstitial fluid. Such approach is derived from the kinetic theory of dense gases [73]. A full derivation of the kinetic energy equation can be found in [41].

In the formulation presented in this section, mass and heat generation due to chemical reactions and radiative heat transfer phenomena are neglected. Mass balance within both phases is represented by the continuity equations defined as:

$$\frac{\partial}{\partial t}\left(\varepsilon_f \rho_f\right) + \frac{\partial}{\partial x_i}\left(\varepsilon_f \rho_f v_{fi}\right) = 0 \tag{2.1}$$

$$\frac{\partial}{\partial t}\left(\varepsilon_s \rho_s\right) + \frac{\partial}{\partial x_i}\left(\varepsilon_s \rho_s v_{si}\right) = 0 \tag{2.2}$$

The first terms on the left-hand side of Eqns. 2.1-2.2 are related to the rate of mass

accumulation per unit volume and the second terms represent the net rate of convective mass flux.

The momentum equations for both phases are expressed as:

$$\begin{aligned}\frac{\partial}{\partial t}\left(\varepsilon_f \rho_f v_{fi}\right)+\frac{\partial}{\partial x_j}\left(\varepsilon_f \rho_f v_{fi} v_{fj}\right) &= -\varepsilon_f \frac{\partial p_f}{\partial x_i}+\varepsilon_f \rho_f g_i+\beta\left(v_{si}-v_{fi}\right) \\ &\quad -\frac{\partial}{\partial x_i}\left(\tau_{fij}\right)-\Gamma_f v_{fi} \end{aligned} \tag{2.3}$$

and

$$\begin{aligned}\frac{\partial}{\partial t}\left(\varepsilon_s \rho_s v_{si}\right)+\frac{\partial}{\partial x_j}\left(\varepsilon_s \rho_s v_{si} v_{sj}\right) &= -\varepsilon_s \frac{\partial p_f}{\partial x_i}+\varepsilon_s \rho_s g_i+\beta\left(v_{fi}-v_{si}\right) \\ &\quad -\frac{\partial}{\partial x_i}\left(\tau_{sij}\right)-\Gamma_s v_{si} \end{aligned} \tag{2.4}$$

where the first and the second terms on the r.h.s are related to buoyancy and gravitational forces. In fluidization model A, the pressure gradient is included in each phase of the momentum equation, however, in model B, the whole gas pressure gradient is applied to the gas phase and the drag function is modified accordingly [74, 38]. The main reason that some researchers use model B is that it makes the set of equations well-posed, however this feature has only been validated for one-dimensional, initial-value problems. The third and fourth terms are, respectively, the interaction force representing the momentum transfer between the fluid and solid phases and the stress tensor. The last term represents the frictional force exerted by the phase *k* on the wall. The thermal energy equations are described as:

$$\begin{aligned}\frac{\partial}{\partial t}\left(C_f \varepsilon_f \rho_f T_f\right) &= -p_f\left[\frac{\partial}{\partial x_i}\left(\varepsilon_f v_{fi}\right)+\frac{\partial}{\partial x_i}\left(\varepsilon_s v_{si}\right)\right]+ \\ &\quad \frac{\partial}{\partial x_i}\left(\varepsilon_f \kappa_f \frac{\partial T_f}{\partial x_i}\right)+\alpha\left(T_s-T_f\right)+\Omega_{wf} \end{aligned} \tag{2.5}$$

$$\frac{\partial}{\partial t}\left(C_s \varepsilon_s \rho_s T_s\right)=\frac{\partial}{\partial x_i}\left(\varepsilon_s \kappa_s \frac{\partial T_s}{\partial x_i}\right)+\alpha\left(T_f-T_s\right)+\Omega_{ws} \tag{2.6}$$

The last three terms on the right-hand side of Eqns. 2.5-2.6 represent the thermal energy transferred by conduction, convection and between phase *k* and the wall, respectively.

The solid fluctuation energy equation is defined for smooth, slightly inelastic and spherical particles as:

$$\frac{3}{2}\left[\frac{\partial}{\partial t}\left(\varepsilon_s \rho_s \Theta\right)+\frac{\partial}{\partial x_j}\left(\varepsilon_s \rho_s v_{s_j} \Theta\right)\right]=\tau_{s_{ij}} \frac{\partial v_{s_i}}{\partial x_j}-\frac{\partial q_j}{\partial x_j}-\gamma-3\beta\Theta \tag{2.7}$$

The granular temperature, Θ, is proportional to the 'granular energy" of the continuum, defined as the specific kinetic energy of the random fluctuating component of the particle velocity:

$$\frac{3}{2}\Theta = \frac{1}{2}\left\langle \overline{C}^2 \right\rangle \tag{2.8}$$

where $\overline{C}$ is the average of the sum of the fluctuating solid velocity components. The second, third and fourth terms on the r.h.s. represent the diffusive flux of granular energy, the rate of granular energy dissipation due to inelastic collisions, and the transfer of granular energy between the fluid and the solid phases.

2.3 Closure-Laws

The conservative equations described in the previous section comprise a number of variables that are specified by specific functions. These functions are established either by fundamental equations or by empirical or experimental correlations. In the following sections, these equations are briefly defined.

2.3.1 Fluid Phase Density

The gas phase, in the equilibrium condition, is assumed compressible and is modelled by the ideal gas equation of state (EOS):

$$p_f = \frac{RT_f}{\overline{V}_f} \tag{2.9}$$

Therefore, gas density is calculated from:

$$\rho_f = \frac{\overline{MW}_f}{RT_f} p_f \tag{2.10}$$

Other equations of state could also be used. However, assuming that the operational conditions are far from the thermodynamical critical coordinates, the ideal gas EOS can be used without introducing further discrepancies.

2.3.2 Drag Coefficient

The momentum transfer between the fluid and the solid phases, β, is usually obtained experimentally from pressure drop measurements. Hence, there are several correlations available in the literature, acquired from fixed or fluidized beds operating with either gas-liquid, gas-solid or solid-liquid systems. In addition, many of these correlations are valid for a fixed range of particle diameter and porosity.

A review of some of these empirical correlations and their applicability can be found in [75]. In this chapter, four correlations are presented, three of them are widely used. Ergun [5] suggested the following equation:

$$\beta = 150\frac{\varepsilon_s^2 \mu_f}{\varepsilon_f d_s^2} + \frac{7}{4}\frac{\rho_f \left|v_f - v_s\right| \varepsilon_s}{d_s} \tag{2.11}$$

However, as this equation is solely valid for a porosity lower than 0.80, Wen and Yu [76] suggested an equation for solid volume fractions in the range 0.1 to 0.63:

$$\beta = \frac{3}{4} C_D \frac{\left(1-\varepsilon_s\right)\varepsilon_s \rho_f \left|v_f - v_s\right|}{d_s}\left(1-\varepsilon_s\right)^{-2.65} \tag{2.12}$$

where the drag coefficient [77], C_D, is related to the dimensionless particle Reynolds number, Re_p, by:

$$C_D = \begin{cases} \dfrac{24}{Re_p\left(1-\varepsilon_s\right)}\left\{1 + 0.15\left[\left(1-\varepsilon_s\right)Re_p\right]^{0.687}\right\} & \text{if } \left(1-\varepsilon_s\right)Re_p < 1000 \\ \\ 0.44 & \text{if } \left(1-\varepsilon_s\right)Re_p \geq 1000 \end{cases} \tag{2.13}$$

Although Wen and Yu used experimental data to correct the interphase transfer momentum coefficient for porosities larger than 0.80, Gidaspow suggested a hybrid equation that used the Ergun equation for solid volume fractions larger than 0.2, and the Wen and Yu equation for porosities larger than 0.8.

$$\beta = \begin{cases} 150\dfrac{\varepsilon_s^2 \mu_f}{\varepsilon_f d_s^2} + \dfrac{7}{4}\dfrac{\rho_f \left|v_f - v_s\right| \varepsilon_s}{d_s} & \text{if } \varepsilon_s > 0.2 \\ \\ \dfrac{3}{4} C_D \dfrac{\left(1-\varepsilon_s\right)\varepsilon_s \rho_f \left|v_f - v_s\right|}{d_s}\left(1-\varepsilon_s\right)^{-2.65} & \text{if } \varepsilon_s \leq 0.2 \end{cases} \tag{2.14}$$

However, this hybrid equation produces a discontinuity in the β-curve at the solid volume fraction value of 0.2 [75]. In order to overcome this discontinuity, Pain et al. [78] suggested another hybrid equation that used Gidaspow's correlation for a range of porosity, and a swarm-corrected single particle drag law for volume fractions less than 0.2, described as follows:

$$\beta = \begin{cases} 150\frac{\varepsilon_s^2 \mu_f}{(1-\varepsilon_s)\, d_s^2} + \frac{7}{4}\frac{\varepsilon_s \rho_f \left|v_f - v_s\right|}{d_s} & \text{if} \quad \varepsilon_s > 0.225 \\ \frac{3}{4} C_D \frac{(1-\varepsilon_s)\, \varepsilon_s \rho_f \left|v_f - v_s\right|}{d_s} (1-\varepsilon_s)^{-2.65} & \text{if} \quad \varepsilon_s \leq 0.175 \\ 20\,(0.225 - \varepsilon_s) \left[150\frac{\varepsilon_s^2 \mu_f}{(1-\varepsilon_s)\, d_s^2} \right. & \\ \left. + \frac{7}{4}\frac{\varepsilon_s \rho_f \left|v_f - v_s\right|}{d_s} \right] + 15\,(\varepsilon_s - 0.175) \times & \\ C_D \frac{\varepsilon_s \rho_f \left|v_f - v_s\right|}{d_s} (1-\varepsilon_s)^{-1.65} & \text{if} \quad 0.175 < \varepsilon_s \leq 0.225 \end{cases} \tag{2.15}$$

2.3.3 Stress Tensor

Gas-phase turbulence has been neglected in the model used in this work due to the uncertainty in turbulence model closures and large gas-phase turbulent suppression in densely packed beds [78]. Either a constant viscosity which equals the gas viscosity is used, or a larger viscosity to act as an eddy viscosity:

$$\tau_{f_{ij}} = 2\varepsilon_f \mu_f \left[\frac{1}{2} \left(\frac{\partial v_{f_i}}{\partial x_j} + \frac{\partial v_{f_j}}{\partial x_i} \right) - \frac{1}{3} \frac{\partial v_{f_k}}{\partial x_k} \right] \tag{2.16}$$

As reported by Enwald [79], while collisional effects have a negligible influence on gas phase flow, the kinetic effect, which consists of the random molecular motion and the mean gas velocity gradient, increases the momentum transferred between the phases. In densely packed beds, the solid stresses are dominated by interparticle friction rather than

by collision or fluctuation motion. Hence, the solid stress tensor is expressed as:

$$\begin{aligned}\tau_{s_{ij}} &= \left(-p_s + \varepsilon_s \zeta_s \frac{\partial v_{s_k}}{\partial x_k}\right)\delta_{ij} \\ &\quad + 2\varepsilon_s \mu_s \left[\frac{1}{2}\left(\frac{\partial v_{s_i}}{\partial x_j} + \frac{\partial v_{s_j}}{\partial x_i}\right) - \frac{1}{3}\frac{\partial v_{s_k}}{\partial x_k}\right]\end{aligned} \tag{2.17}$$

This equation takes into account particle collisions and slidings effect, as described by the Coulomb criteria [80, 81, 82, 72, 83, 84].

2.3.4 Solid Phase Pressure

The solid pressure, p_s, represents the solid-phase normal forces due to particle-particle interactions and can be written in two parts, a kinetic contribution and a collisional contribution:

$$p_s = \varepsilon_s \rho_s \Theta + 2\nu \varepsilon_s^2 \rho_s \Theta \left(1 + e_{pp}\right) \tag{2.18}$$

where ν, the radial distribution function, is defined in Section 2.3.9, and e_{pp} is the particle-particle collisional coefficient. The kinetic part, expressed by the first term on the r.h.s., is due to the momentum transferred by the shear stress caused by the flow of particles, and the second term, related to the collisional contribution, is due to the momentum transferred between particle collisions.

2.3.5 Solid Shear Viscosity

Several empirical correlations were developed to calculate the solid shear viscosity, ζ_s. Most of them converge for densely packed beds, however they differ in dilute regions [75]. In this work, the following equation was used:

$$\zeta_s = \frac{4}{5}\varepsilon_s \rho_s d_s \nu \left(1 + e\right)\sqrt{\frac{\Theta}{\pi}} \tag{2.19}$$

2.3.6 Solid Bulk Viscosity

The solid bulk viscosity can be defined as the resistance of the particle suspension against compression [85], and expressed as:

$$\mu_s = \frac{4}{3}\varepsilon_s \rho_s d_s \nu \left(1 + e\right)\sqrt{\frac{\Theta}{\pi}} \tag{2.20}$$

2.3.7 Interphase Heat Transfer

The interphase heat transfer mechanism is related to the temperature gradient between a theoretical fluid-layer alongside a surface and the surface itself. The volumetric interphase heat transfer coefficient, α, is defined for uniformly-sized spherical particles as:

$$\alpha = \frac{6\varepsilon_g}{d_s} h_{fs} \tag{2.21}$$

Several empirical correlations were proposed to calculate the fluid-particle heat transfer coefficient, h_{fs}. In this work, the empirical correlation introduced by Gunn [56] was used. This equation calculates the Nusselt dimensionless number, Nu, as a function of the local flow dynamics, represented by the particle Reynolds number (Re_p), and the thermophysical properties of the fluid phase, expressed by the Prandtl number, Pr:

$$Nu = \frac{h_{fs} d_s}{\kappa_f} = \left(7 - 10\varepsilon_f + 5\varepsilon_f^2\right)\left(1 + 0.7 Re_p^{1/5} Pr^{1/3}\right) + \left(1.33 - 2.4\varepsilon_f + 1.2\varepsilon_f^2\right) Re_p^{0.7} Pr^{1/3} \tag{2.22}$$

This equation is valid for a porosity in the range from 0.35 to 1.00. The use of this empirical equation introduces some inaccuracies. However, as the volumetric heat transfer coefficient becomes larger, the temperature difference between the phases remains small, and this inaccuracy can be considered negligible.

2.3.8 Wall-Bed Heat Transfer

As bubbles rise through the domain, particles fall near the wall region replacing hot particles which ascend in the rear of bubbles. Such dynamics are responsible for the thermal energy transferred from the heat exchange surface to the granular phase. In this case, the heat transfer coefficient can be calculated as

$$h_{ws} = 2\frac{\varepsilon_s \kappa_s}{d_s} \tag{2.23}$$

Equation 2.23 is a simplified version of the wall-bed with stagnant gas heat transfer equation [4] and is related to the heat flux from the surface into the particle-fluid layer with thickness of $d_s/2$ in contact with it. In this work, the wall-gas phase heat transfer is considered negligible.

2.3.9 Thermal Conductivities

The conductive mechanism is concerned with the thermal diffusion through a phase. In the fluid phase, the conduction is a function of the thermophysical properties alone, whereas in the solid phase, the inter-particle collisions time contact is an additional influence. In this section, three approaches are presented. In Chapter 3, a few numerical simulations in bubbling fluidized beds using these approaches are compared.

The first approach (referred to henceforth as the *standard approach*) is based on Zeher and Schlunder's work [65]. They calculated the conductivity coefficient in a bulk of particles and fluids. However, in order to transpose this approach to the Eulerian-Eulerian description, the gas and particle conductivities should be split into phases, as described by Syamlal and Gidaspow [86] and Kuipers *et al.* [63]. Hence, the fluid phase conductivity can be defined as:

$$\kappa_f^* = \varepsilon_f \kappa_f = \left(1 - \sqrt{1-\varepsilon_f}\right) \kappa_{gas} \tag{2.24}$$

For the solid phase, the following set of equations are used to calculate the so-called *solid phase effective conductivity*, $\varepsilon_s \kappa_s$ (a full description can be found in [63, 65]):

$$\kappa_s^* = (1-\varepsilon_f)\,\kappa_s = \sqrt{1-\varepsilon_f}\,[\vartheta \kappa_{sol} + (1-\vartheta)\,\Xi] \tag{2.25}$$

where:

$$\Xi = \frac{2\kappa_{gas}}{1-\overline{\kappa}} \left[\frac{(1-\overline{\kappa})\,\chi}{(1-\overline{\kappa}\chi)^2}\right] \ln(\chi\overline{\kappa}) - \frac{\chi+1}{2} - \frac{\chi-1}{1-\overline{\kappa}\chi} \tag{2.26}$$

with:

$$\chi = 1.25\left(\frac{1-\varepsilon_f}{\varepsilon_f}\right)^{10/9} \;;\; \overline{\kappa} = \frac{\kappa_{gas}}{\kappa_{sol}} \text{ and } \vartheta = 7.6 \times 10^{-3}$$

Another method of obtaining the thermal conductivity of the solid phase is to assume it as a function of the granular temperature. One of the major advantages of this approach over the standard approach is its consistency with the overall model, which uses the kinetic theory to model the granular behavior. Analogous to the gas kinetic theory [73], the energy stored in a gas, is diffused by the exchange of kinetic energy between its molecules, expressed by the thermal conductivity. Similarly, from the particle kinetic theory of dense flows, the kinetic energy is transferred by the collision between particles. Hence, the thermal conductivity of the solid phase is due to the collisions and the velocity fluctuations, both of which are strongly influenced by the change in the thermodynamic temperature.

Several empirical and theoretical equations have been developed to calculate the effective thermal conductivity, $\varepsilon_s \kappa_s$. A noteworthy review of some of them can be found in [75]. Hunt [66] derived the thermal conductivity as a function solely of the kinetic energy of random particle fluctuations:

$$\kappa_s^* = \varepsilon_s \kappa_s = \varepsilon_s \rho_s C_s d_s \frac{\sqrt{\pi \Theta}}{32\nu} \tag{2.27}$$

where ν is the radial distribution function, defined in [66, 75] as:

$$\nu = \left[1 - \left(\frac{\varepsilon_s}{\varepsilon_s^{mp}} \right) \frac{1}{3} \right]^{-1} \tag{2.28}$$

and ε_s^{mp} is the particle volume fraction at maximum packing. The radial distribution function, ν, is related to the Maxwellian distribution of the probability of finding N particles of diameter d_s in a volume control with a given fluctuation velocity, i.e., it describes the probability of interparticle collisions.

Natarajan and Hunt [68] introduced another correlation, based on the works of Gelperin and Einstein [5] and Hsiau and Hunt [67] which takes into account both streaming or kinetic factors and molecular or collisional (i.e., due solely to thermophysical properties) factors. According to them, both factors, when applied to low-density and highly sheared flows, act in opposition, i.e., by decreasing the solid volume fraction, which allows the particles to stream across larger distances and raise the effective conductivity. However, by increasing the solid volume fraction, the conductivity due to collisional effects is increased by enhancing the proximity of particles and the probability of collisions. Therefore, energy is dissipated due to these inelastic collisions and to frictional interactions between the particles and the particles and the walls.

$$\begin{aligned} \kappa_s^* = \varepsilon_s \kappa_s \quad = \quad & \frac{\left(\varepsilon_s \rho_s C_s + \varepsilon_f \rho_f C_f \right) d_s \sqrt{\frac{\Theta}{\pi}}}{9 \left(1 - \varepsilon_f \right) \nu} + \\ & \kappa_{gas} \left[1 + \frac{\varepsilon_s \left(1 - \overline{\kappa} \right)}{\overline{\kappa} + 0.28 \left(1 - \varepsilon_s \right)^{0.63\overline{\kappa} - 0.18}} \right] \end{aligned} \tag{2.29}$$

where, in this case, the radial distribution function is expressed as:

$$\nu = \left(\frac{1 - \varepsilon_s}{\varepsilon_s^{mp}} \right)^{-2.5 \varepsilon_s^{mp}} \tag{2.30}$$